Energy Transfer in the Inhomogeneously Broadened Core Antenna of Purple Bacteria: A Simultaneous Fit of Low-Intensity Picosecond Absorption and Fluorescence Kinetics

Tõnu Pullerits,* Kees J. Visscher,* Sussan Hess,* Villy Sundström,* Arvi Freiberg,§ Kõu Timpmann,§ and Rienk van Grondelle¶

*Department of Physical Chemistry, University of Umeå, Umeå, Sweden; §Institute of Physics, Estonian Academy of Sciences, Tartu, Estonia; and ¶Department of Physics and Astronomy, the Free University of Amsterdam, Amsterdam, the Netherlands

ABSTRACT The excited state decay kinetics of chromatophores of the purple photosynthetic bacterium *Rhodospirillum rubrum* have been recorded at 77 K using picosecond absorption difference spectroscopy under strict annihilation free conditions. The kinetics are shown to be strongly detection wavelength dependent. A simultaneous kinetic modeling of these experiments together with earlier fluorescence kinetics by numerical integration of the appropriate master equation is performed. This model, which accounts for the spectral inhomogeneity of the core light-harvesting antenna of photosynthetic purple bacteria, reveals three qualitatively distinct stages of excitation transfer with different time scales. At first a fast transfer to a local energy minimum takes place (≈1 ps). This is followed by a much slower transfer between different energy minima (10–30 ps). The third component corresponds to the excitation transfer to the reaction center, which depends on its state (60 and 200 ps for open and closed, respectively) and seems also to be the bottleneck in the overall trapping time.

An acceptable correspondence between theoretical and experimental decay kinetics is achieved at 77 K and at room temperature by assuming that the width of the inhomogeneous broadening is 10–15 nm and the mean residence time of the excitation in the antenna lattice site is 2–3 ps.

INTRODUCTION

The absorption of a light quantum by the photosynthetic light-harvesting antenna initiates a sequence of very fast kinetic processes. These include the transfer of the singlet electronic excitation through an array of antenna light-harvesting pigment protein complexes (LHC) to the reaction center (RC) pigment-protein complex, where separation of charges takes place.

The energy transfer processes in antenna systems have been extensively studied (for reviews see Van Grondelle, 1985; Sundström and Van Grondelle, 1991; Holzwarth, 1991). However, different backtransfer reactions and overlapping spectra mix the elementary energy transfer steps in a complex way and consequently a straightforward interpretation of experimental results is in most cases impossible. Therefore, a number of kinetic models have been developed on various levels of approximation, each of which has contributed to our increasing understanding of the different aspects of energy transfer (Seely, 1973; Shipman, 1980; Pearlstein, 1982; Den Hollander et al., 1983; Kudzmauskas et al., 1983; Fetisova et al., 1985; Källebring and Hansson, 1991).

Unfortunately, for most photosynthetic systems little is known at the molecular level about the structural organization of the antenna pigments. One of the few exceptions is the bacteriochlorphyll (Bchl) *a*-protein of *Prostechochloris aestuarii*, but even in that case, a more or less satisfactory calculation of its steady-state spectra has only recently appeared (Pearlstein, 1992a), despite the fact that structural information has been available for this protein for over 15 years. Thus, even very detailed structural information on a photosynthetic pigment-protein complex does not necessarily allow a complete picture of the excitation transfer dynamics.

It is generally accepted that most of the photosynthetic antennas are spectrally heterogeneous. "Heterogeneity" means that the absorption spectrum of a particular photosynthetic species consists of several bands with different spectral properties. As a rule spectrally different groups of LHCs are organized in such a way that an energy gradient is created that efficiently drives the excitation energy toward the RC (see, e.g., Duysens, 1986). For example, one of the simplest photosynthetic organisms, the Bchl *a*-containing purple bacterium *Rhodospirillum (R.) rubrum*, is characterized by a single broad absorption band in the near infrared (termed B880 after its long wavelength Q_y absorption peak) and thus is believed to have only a single membrane-embedded spectral form of LHC. On the other hand, *Rhodobacter (Rb.) sphaeroides* exhibits a more heterogeneous absorption spectrum with peaks at 800, 850, and 875 nm. The former two are ascribed to a peripheral LHC (B800–850), while the 875 band, which is functionally the same as the B880 band in *R. rubrum*, belongs to the core antenna (LH1) that surrounds the RC.

Besides this heterogeneity, the concept of spectral inhomogeneity has been introduced to photosynthetic antennae (Freiberg et al., 1987, 1989). Heterogeneity is the result of large scale systematic differences in the chemical surroundings of pigment molecules (e.g., due to binding to different polypeptides or binding to different parts of a polypeptide

Received for publication 22 June 1993 and in final form 29 September 1993.

Address reprint requests to Dr. Villy Sundström, Department of Physical Chemistry, University of Umeå, S-901 87 Umeå, Sweden.

0006-3495/94/01/236/13 $2.00

chain), whereas inhomogeneity is caused by stochastic fluctuations (e.g., small differences in the positions and directions of sidegroups, small fluctuations in the H-bonding pattern) of the surroundings. Thus, heterogeneity has a discrete nature and the position of the absorption band is correlated with the spatial location of that particular spectral type of pigment in the photosynthetic system, while inhomogeneity implies a continuous distribution of transition energies without any correlation between location and spectrum. This kind of spectral inhomogeneity seems to be a universal property of complex biological systems (Ormos et al., 1990).

Recently several models have been developed addressing the relation between spectral inhomogeneity and energy transfer dynamics. Valkunas et al. (1992) have presented a simple kinetic model for *R. rubrum*, which enables a qualitative understanding of the role of spectral inhomogeneity. Van Mourik et al. (1992) have simulated the 4 K site-selected emission spectra in terms of energy transfer in a cluster of weakly coupled pigments. Each individual cluster is supposed to be a random sample from the inhomogeneous distribution of pigments. Within each cluster fast energy transfer was assumed to take place from the "blue" to the "red" pigments. Jean et al. (1989) and Beauregard et al. (1991) presented simulations of excitation transport and trapping on spectrally disordered lattices with a finite number of spectral forms based on a numerical solution of the Pauli master equation. Jia et al. (1992) improved the previous model of Jean et al. (1989) by including the temperature dependence of the microscopic transfer step by calculating the absorption and emission spectra of the individual pigments in the protein matrix using a model Hamiltonian which includes a phonon contribution. In this approach the temperature dependence of the spectra arises from the thermal population of the low frequency modes, which broaden the absorption/emission spectra of the spectral components.

Pullerits and Freiberg (1991, 1992) and Freiberg and Pullerits (1990) developed a model addressing the experimentally observed detection wavelength dependence of the fluorescence kinetics in the inhomogeneously broadened antenna of *R. rubrum* (Freiberg et al., 1987; Timpmann et al., 1991). A number of computer "experiments" have been carried out and a reasonably good agreement between theoretical and experimental kinetics has been demonstrated both at 77 K and at ambient temperatures assuming a rather large hopping time, defined as the average time of excitation transfer between two antenna molecules. This slow hopping is in contradiction to the room temperature hopping time that was extracted from singlet-singlet annihilation measurements (Bakker et al., 1983; Vos et al., 1986; Deinum et al., 1989); it is also inconsistent with the fast ($\ll$10 ps) and efficient depolarization of the antenna excited states observed in picosecond absorption anisotropy measurements (Sundström et al., 1986; Van Grondelle et al., 1987). However, in a recent paper Van Mourik et al. (1993) pointed out that energy transfer in a large spectrally inhomogeneous system occurs on two time scales: a fast hopping toward a local minimum followed by a slow transfer between local minima. For a small photosynthetic unit (PSU) that is not representative of the total inhomogeneous distribution the second process is not observed. Consequently, the "slow" decay measured in the fluorescence was possibly confused with the initial localization process, leading to an overestimation of the hopping times.

In this article we have further investigated this problem by application of the model of Pullerits and Freiberg (1992) simultaneously to new absorption and earlier fluorescence kinetics data. We have extended the previous model by assuming that the unit cell in the calculation is an assembly containing several PSUs. This new aspect has enabled us to overcome the above-mentioned controversy and resulted in a good correspondence between the computer model fits and both pump-probe and time-resolved fluorescence experiments.

MATERIALS AND METHODS

Experimental

Previous one-color pump-probe measurements on *R. rubrum* at 77 K (Van Grondelle et al., 1987) have clearly shown that upon exciting and probing in the blue wing of the LH1 absorption spectrum, fast ($\approx$10 ps) decay components are observed. Red-edge excitation and probing resulted in close to monoexponential decay. The fast component was interpreted as fast energy transfer from blue-absorbing to red-absorbing pigments: B880 $\rightarrow$ B896 energy transfer within the two-state model of the LH1 antenna. In the present measurements we use independently tunable pump and probe wavelengths, which enables us to excite pigments in the blue part of the LH1 absorption spectrum and monitor the excited state decay (i.e., ground state bleaching) of the red-absorbing pigments. This was done by exciting the LH1 antenna at 870 nm and probing the decay and formation of excited states at several wavelengths in the range of 887 to 900 nm.

All measurements were performed on chromatophores of *R. rubrum* at 77 K with photochemically inactive reaction centers P^+IQ (P is the primary electron donor, a Bchl *a* dimer; I is the intermediate electron acceptor, a bacteriopheophytin; and Q is the primary quinone acceptor). This redox state of the RC is maintained by the high pulse repetition rate of the laser, when no artificial electron donors are added to the sample. P^+ is known to efficiently quench the antenna excitation energy with a time constant of 200–250 ps (Sundström et al., 1986; Freiberg et al., 1989). Two trains of independently tunable picosecond pulses were generated by pumping in parallel two dye lasers with a mode-locked and frequency-doubled continuous wave Nd^{3+}-YAG laser operating at 80 MHz. The pulse repetition rates of the two dye lasers were reduced to 80 kHz by cavity dumping, and the two pulse trains were synchronized by using one of the cavity dumper drivers as master oscillator for the other one. In this way a timing jitter between the two pulse trains of less than 2 ps was accomplished, and a cross-correlation pulse of $\approx$12 ps was obtained. With the dye Styryl 9 both dye lasers could be independently tuned over the wavelength interval 790–920 nm. The low repetition rate and the reduced peak power were sufficient to avoid singlet-singlet and singlet-triplet annihilation in these experiments. The chromatophores used in the absorption measurements were prepared as previously described from wild type *R. rubrum*.

The details of the fluorescence experiment were published elsewhere (Timpmann et al., 1991).

Model

Here we shall present the essentials of the model; the interested reader is referred to the original paper (Pullerits and Freiberg, 1992) where all details are given.

The Förster-type incoherent energy transfer is assumed to take place in a two-dimensional antenna lattice and is described by the Master equation:

$$\begin{cases} \dot{p}_i = \sum_{j=1}^{N} (p_j W_{ji} - p_i W_{ij}) - \frac{p_i}{\tau_l} - \delta_{1i}\left(\frac{p_1}{\tau_{RC}} - \frac{p_0}{\tau_{RC}}\right) \\ \dot{p}_0 = \frac{p_1}{\tau_{RC}} - p_0\left(\frac{f}{\tau_{RC}} + \frac{1}{\tau_Q}\right). \end{cases} \quad (1)$$

Here p_i is the probability that an excitation is at antenna site i; p_0 denotes the radical pair P^+I^- state and p_1 is the RC special pair excited state. $N-1$ is the number of LHCs in a PSU, τ_l is the time of excitation decay due to all losses in the antenna except quenching by RC, δ_{ij} is the Kronecker delta. τ_{RC} is the primary charge separation time in the RC. τ_Q is the time required for the process $P^+I^- \rightarrow P^+IQ^-$ and $f = \exp(-\Delta E_{RC}/kT)$, where ΔE_{RC} is the free energy difference between the states P* and P^+I^-, k is the Boltzmann constant, and T is the absolute temperature. W_{ij} is the rate of excitation transfer from site i to site j. The quenching by closed RCs is simulated by the irreversible excitation transfer from antenna to P^+ (we let $\tau_{RC} \rightarrow 0$).

The original Förster formula (Förster, 1965) and formulae derived from it (Jean et al., 1989; Beauregard et al., 1991; Pullerits and Freiberg, 1991) contain a number of uncertain parameters. Problems with the Förster radius and the natural lifetime (transition dipole strength) of the pigments have been discussed by Pullerits and Freiberg (1992). The refractive index occurs in the fourth power and even the applicability of this macroscopic constant on a microscopic level is not obvious. To avoid these problems the distance between pigments is commonly adjusted to get the correct transfer rate. Of course, such a "determination" of the lattice constant should be made with caution and makes sense only if independent and reliable structural information is available, as for the chlorophyll *a/b* complex (Kühlbrandt and Wang, 1991) or the core antenna of photosystem I (PSI) (Krauss et al., 1993).

Pullerits and Freiberg (1992) have included all above-mentioned uncertain parameters into the so-called resonant pairwise transfer time τ_{tf}, which is one of the model parameters estimated from the comparison with experiment. Following this self-consistent empirical approach we have:

$$W_{ij} = \frac{3}{2}\chi_{ij}^2 \frac{\theta_{ij}(\nu_{ij}, T)a^6}{\tau_{tf}(0, T_0)r_{ij}^6}. \quad (2)$$

The distance between lattice sites i and j, r_{ij}, can be written as the lattice constant a multiplied by a constant determined by the mutual position of sites i and j and the structure of the lattice. $\theta_{ij}(\nu_{ij}, T)$ is the spectral overlap between donor and acceptor with energy gap ν_{ij} at temperature T relative to the resonant ($\nu_{ij} = 0$) overlap at temperature T_0. ν_{ij} is determined as a difference between 0-0 transition positions of sites i and j.

$$\chi_{ij}^2 = \cos\alpha_{ij} - 3\cos\beta_{ij}\cos\gamma_{ij}. \quad (3)$$

α_{ij} is the angle between the transition dipole moments of the donor i and the acceptor j; β_{ij} and γ_{ij} are the angles between each dipole and the vector connecting them.

In the case of multiphonon transitions (at temperatures above or around the Debye temperature, for organic molecular systems ≥100 K), the homogeneous spectra are well approximated by Gaussian shapes (Rebane, 1970), and we get:

$$\theta_{ij}(\nu_{ij}, T) = \frac{\sigma_{ij}^h(T_0)}{\sigma_{ij}^h(T)} \exp\left[-\frac{1}{2}\left(\frac{(\nu_{ij} - S_{ij})^2}{\sigma_{ij}^h(T)^2} - \frac{S_{ij}^2}{\sigma_{ij}^h(T_0)^2}\right)\right], \quad (4)$$

where $\sigma_{ij}^h(T)^2 = \sigma_i^h(T)^2 + \sigma_j^h(T)^2$, $S_i = (S_i + S_j)/2$. The temperature-dependent full width of the homogeneous spectra of site i at half-maximum intensity (FWHM) is derived as $\Delta_i^h(T) = \sqrt{2\ln 2}\,\sigma_i^h(T)$. S_i is the homogeneous Stokes shift.

Note that S_i cannot be measured directly from the antenna spectra as the difference between the fluorescence and the absorption maximum because, due to the energy transfer, the maximum of the fluorescence spectrum is shifted to the red, and this may lead to remarkable mistakes. It should rather be calculated using the expression given by Pullerits and Freiberg (1991) from the temperature-dependent experimentally observable FWHM of an inhomogeneously broadened absorption band, which is a convolution of the homogeneous absorption spectrum of site i with the distribution function of electronic transition energies of the sites (the inhomogeneous distribution function (IDF)). In that way we have estimated $S_i = 10$ nm (110 cm^{-1}) for the antenna.

The temperature dependence of homogeneous bandwidths in the case of multiphonon spectra is given by (Osad'ko, 1979):

$$\sigma_i^h(T)^2 = \sigma_i^h(0)^2 + 2kTS_i, \quad (5)$$

in which the temperature-independent constant $\sigma_i^h(0) \ll kTS_i$ if $T \gg 0$.

We assume that all sites $\sigma_i^h(T)$ and S_i, which belong to a single inhomogeneous spectral type of LHC (e.g., B880 in *R. rubrum*), have the same values, but different from those of the RC site. In the case of a heterogeneous antenna (e.g., B800–850 and B875 of *Rb. sphaeroides*), these parameters may be different for the various antenna spectral forms as well.

Most of the model parameters can be fixed thanks to the availability of independent and reliable experimental data. All these have been systematically presented and discussed by Pullerits and Freiberg (1992) and we are not going to repeat them here. The only three parameters left, which one has to estimate from a comparison with the experiment assuming a specific PSU structure, are the resonant pairwise transfer times between neighboring antenna sites τ_{tf}^a and from antenna site to RC τ_{tf}^{RC} and the FWHM of the antenna IDF, Δ_0.

The Master equation (Eq. 1) is solved by using the Green function method, which gives the excitation dynamics as a sum of exponents. After averaging over possible spectral conformations we write it in a more generalized way (Pullerits and Freiberg, 1992):

$$p(\lambda_{ex}, \lambda_{rec}, t) = \int_0^\infty \rho(\lambda_{ex}, \lambda_{rec}, \tau)\exp(-t/\tau)\,d\tau, \quad (6)$$

where $p(\lambda_{ex}, \lambda_{rec}, t)$ and $\rho(\lambda_{ex}, \lambda_{rec}, \tau)$ are the absorption/fluorescence kinetics and a distribution of amplitudes of decay constantants, respectively, recorded at λ_{rec} in the case of excitation at wavelength λ_{ex}.

This approach enables us to calculate the dependence of the distributions of decay constants on the exciting and recording wavelength for both transient absorption and fluorescence measurements.

SIMULATIONS AND COMPARISON WITH EXPERIMENT

Cyclic boundary conditions

In most of the photosynthetic organisms, the photosynthetic apparatus is embedded into a flat cytoplasmic membrane where energy transport takes place mainly in two dimensions. Moreover, excitation annihilation experiments have shown that the excitation may visit several (≥10) PSUs before being lost or trapped (Bakker et al., 1983; Van Grondelle, 1985). Thus, the system can be considered as a large array of PSUs. If all PSUs are equivalent, the energy transfer in this system can be found by applying periodic boundary conditions to a single PSU, and performing the calculations for one PSU, as has been done by Pullerits and Freiberg (1992).

However, in our case PSUs are actually not identical since each of them represents a random sample from IDF. The applicability of periodic boundary conditions in that case depends on how well a single PSU represents the whole distribution. To investigate this point we made simulations in which the unit cell was chosen to consist of two, three, and four PSUs put together, the periodic boundary conditions were applied to these larger units, and the results are shown

in Figs. 1 and 2. For the unit cells consisting of more than one PSU a new feature appears in the lifetime distribution that represents a decay process with a lifetime approximately 1 order of magnitude longer than the mean residence time of the excitation on the antenna lattice site τ_h defined as τ_{tf}^a divided by the number of the nearest neighbors ("mean" denotes here the statistical nature of the excitation localization time on a molecule, not the average over the spectral inhomogeneity). For instance, for $\tau_h = 2$ ps, the new decay component has a maximum around 30 ps with some amplitude up to 100 ps (see Figs. 1 and 2). A 2-fold increase (decrease) in τ_h increases (decreases) also the position of the maximum of this slower process by approximately the same factor. We stress here that this feature is present only if calculations are done for a unit cell containing several coupled PSUs. The shape (maximum, width) of the lifetime distribution is quite insensitive to the number of PSUs, but the amplitude increases rapidly with the number of PSUs for unit cells containing up to three PSUs. The differences between calculations with three and four PSUs as the elementary unit were negligible at 77 K, and all the following calculations were done with three PSUs.

The possibility of missing some details of the transfer kinetics using periodic boundary conditions was recently discussed by Van Mourik et al. (1993) based on the papers of Ries et al. (1988), which have shown that strong inhomogeneity causes a separation of the time scales of the energy transfer process into two categories. The initial transfer is very fast, since it concerns mainly downhill transfer among neighboring pigments until a local energy minimum is reached. After this first initial phase, the further rate of diffusion of the excitation is strongly reduced.

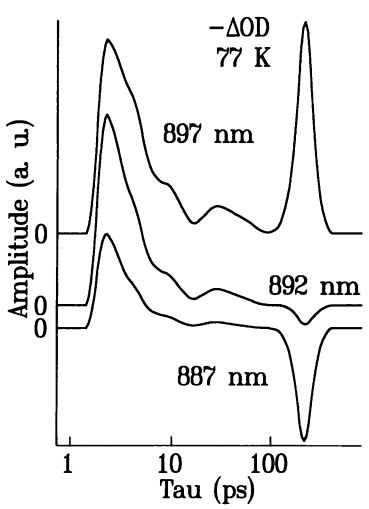

FIGURE 1 Distributions of amplitudes of absorption decay constants $\rho(\lambda_{ex}, \lambda_{rec}, \tau)$ (see Eq. 6) at three different recording wavelengths in case of closed RCs at 77 K. The negative amplitude appears as a rising component in the decay curves. Excitation into blue edge of the absorption band. λ_{exc} = 870 nm. τ_{tf}^a = 15 ps, which corresponds to a mean residence time on an antenna lattice site of about 3 ps, Δ_0 = 10 nm (120 cm^{-1}), τ_{tf}^{RC} = 30 ps. Calculations are performed with three PSUs. The band around 30 ps disappears if calculations are performed with one PSU as an elementary unit. The longest decay component around 200 ps corresponds to the trapping by closed RCs. The lattice structure number one (see Fig. 5) is used.

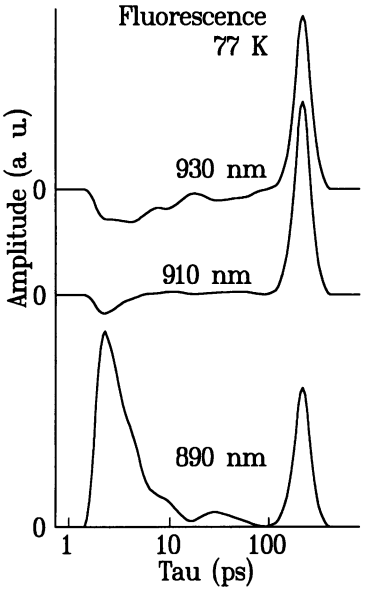

FIGURE 2 The same as Fig. 1 but now for the fluorescence.

Pullerits and Freiberg (1992) checked this point also, comparing "correct" kinetic traces from Monte Carlo random walk calculations with traces from Master equation simulations (for one PSU as a unit cell and with periodic boundary conditions). The differences were found to be of the order of the noise in Monte Carlo calculations. The reason for this is most likely the fundamental fallacy in comparing noisy decay curves with the sum of exponentials (James et al., 1985).

Structure

In contrast to the bacterial RC, x-ray diffraction data with high resolution of antenna complexes of purple bacteria are not available so far, and most information about their organisation is gathered from biochemical and spectroscopic studies. It is estimated that in the PSU of *R. rubrum* there are ≈24 Bchl *a* antenna molecules per RC (Chang et al., 1990). It has been found that the *R. rubrum* B880 LHCs could be reversibly dissociated into the so-called B820 subunit form (Miller et al., 1987). Spectroscopic measurements on the B820 subunit (Van Mourik et al., 1991; Visschers et al., 1991; Visschers, 1993) have given a strong indication that the basic building block of the antenna is a strongly coupled dimer of Bchl *a*. A study of reassociation of these subunits (Van Mourik, 1993) suggests the reaction scheme 2 B820 → B873, the latter having very similar properties to the in vivo LH1. At the same time neither triplet minus singlet spectra (Van Mourik et al., 1993) nor the circular dichroism spectra (Kramer et al., 1984a) of the LH1 antenna indicate a significant increase in the exciton splitting, which shows that most of the dimeric character of the B820 is maintained in the LH1. Consequently, even if the structural unit of the (re)associated LH1 is an oligomer of four pigments

(Meckenstock et al., 1992a), it is likely to be a weakly coupled aggregate of two dimers of strongly coupled Bchl *a* molecules (Van Mourik, 1993).

On the other hand, Gingras and Picorel (1990) have estimated from radiation inactivation and electron paramagnetic resonance studies of *R. rubrum* core antenna complexes that the hexameric aggregates of protein α,β-polypeptide pairs, binding 12 Bchl *a* molecules, form close assemblies. At the same time these authors showed further evidence for the dimeric nature of B880 (Picorel et al., 1986). Recently also Boonstra et al. (1993) have concluded from the electron microscopy studies of core antenna of *Rb. sphaeroides* that the B875 complexes have a diameter of 52 Å and are most likely to have a 6-fold symmetry consisting of six α,β-pairs forming a ring-like structure. The inner diameter of the ring seems not sufficient to contain the RC.

All these studies were done with RC-less objects. We have no evidence whether or not the RC has an organizing influence on the *R. rubrum* LH1 structure. In another bacterium, *Rhodopseudomonas (Rps.) marina*, electron microscopic studies (Meckenstock et al., 1992b) revealed cyclic structures with a diameter of 102 Å for both membranes with RCs and RC-less B880 antenna complexes. In membranes the RCs are situated at the centers of the rings. A similar structure was reported earlier for *Rhodopseudomonas viridis* by several groups (Miller, 1982; Welte and Kreutz, 1982; Stark et al., 1984; Ghosh and Bachofen, 1989). In conclusion, ring-like structures seem to be favored for the LH1-RC core, but other aggregation forms cannot be excluded.

Recently it has been pointed out that a so-called monocoordinate model (Zhang et al., 1992; Pearlstein, 1992b) may be a good description of the antenna-RC contact in *Rps. viridis*. In that case the transfer to the RC takes place mainly from the single antenna site, which is closest to the RC (distance is equal to the lattice constant). Some support for this idea originates from the orientational factor χ^2, which occurs in the Förster formula (Eq. 2). We have performed Monte Carlo simulations to calculate the probability density $P(\chi^2)$ of all possible χ^2 values from 0 to 4 if the donor and acceptor transition dipole moments are assumed to be oriented randomly in either three or two dimensions. $P(\chi^2)d\chi^2$ gives the probability that χ^2 occurs in the infinitesimal interval between χ^2 and $\chi^2 + d\chi^2$. The corresponding density curves are given in Fig. 3 *A*. It is remarkable that in the case of randomly oriented dipoles in space half of the possible conformations have an orientation factor <0.4, which means 1 order of magnitude less than the maximum possible value 4. Both the RC special pair (Breton, 1985) and LH1 antenna (Kramer et al., 1984b) transition dipole moments are oriented parallel to the membrane plane. It is clear from Fig. 3 *A* that keeping transition dipole moments oriented in a plane avoids a large number of possible unfavorable conformations with $\chi^2 < 1$. We also point to the peculiarities of the curves at $\chi^2 = 1$, the origin of which can be understood with the help of Fig. 3 *B*. For the least favorable case (a pigment

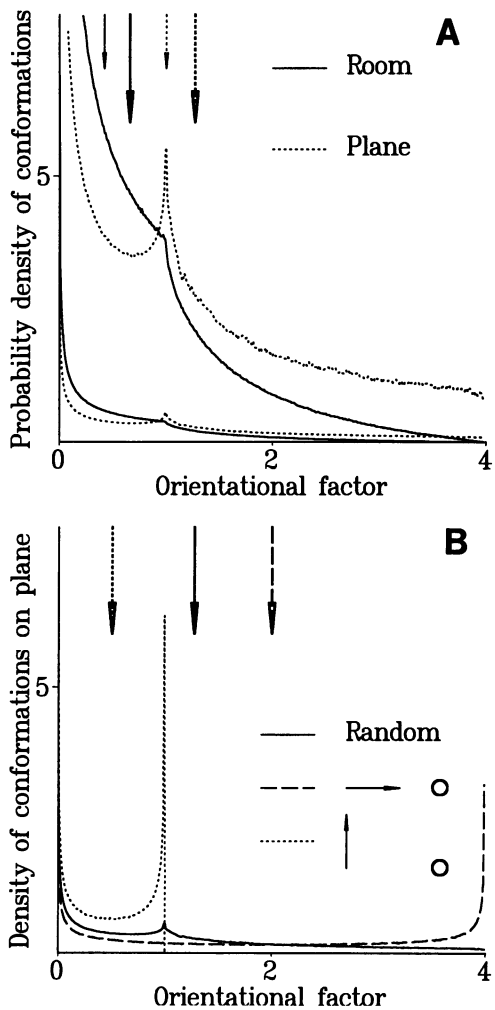

FIGURE 3 Probability density P of the orientational factor χ^2. $P(\chi^2)d\chi^2$ gives the probability that χ^2 occurs in the interval between χ^2 and $\chi^2 + d\chi^2$. (*A*) Two transition dipole moments are random in space or on a plane. The same curves are with 10 times different scalings. Long arrows indicate the mean values of orientational factors (the first moments); short arrows give the corresponding centers of the probabilities. (*B*) Transition dipoles are on a plane. The solid curve is a reference from *A* with both dipoles random on a plane. The other two curves give the case if one molecule has a random dipole-moment orientation and the dipole-moment of another molecule is fixed either in the direction parallel to the line connecting two molecules (*dashed curve*) or fixed in the direction perpendicular to that line (*dotted curve*). Arrows give the mean values of the orientational factors of corresponding distributions.

with a random dipole-moment orientation situated in the way that the line which connects the molecules is perpendicular to the dipole-moment of the fixed molecule; see also the caption to Fig. 3), χ^2 has values from 0 to 1 (*dotted curve*). On the other hand, in the most favorable case (the line which connects the molecules is parallel to the dipole-moment of the fixed molecule; *dashed curve*) χ^2 extends up to 4. Now one can think about the two-dimensional χ^2 probability curve of Fig. 3 *A* as a weighted average of all possibilities from the above-mentioned least favorable to the most favorable case, and this is the origin of the maximum of the two-dimensional χ^2 probability

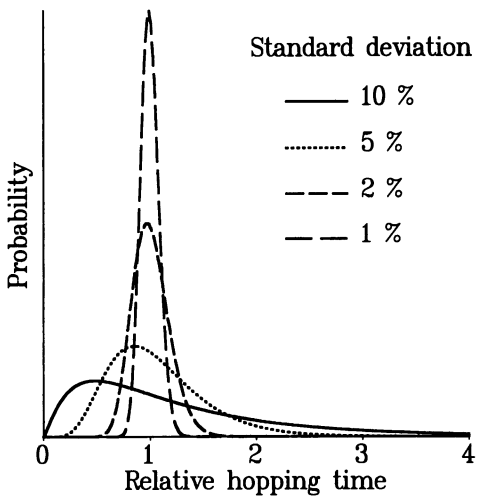

FIGURE 4 The distribution of the hopping time in a distorted lattice relative to the hopping time in the perfect lattice. We are using the hopping times in the sense of the reciprocal of the transfer rate, thus omitting its statistical nature even in the case of the perfectly ordered lattice. The coordinates of the distorted lattice sites have been left to fluctuate randomly according to Gaussian distribution around the ideal lattice site with different deviations of the distribution—1, 2, 5, and 10% of the lattice constant.

density at $\chi^2 = 1$. Analogously, in the three-dimensional case we get a shoulder at that point. Finally, it can be seen from Fig. 3 *B* that the excitation transfer rate for pigments positioned in the direction of dipole moment (*dashed density curve*) is on the average 4 times larger in comparison to the transfer rate from the pigments that are positioned in a direction perpendicular to the special pair dipole orientation (*dotted curve*). Such an enhancement of the transfer rate for some selected antenna molecules is analogous to the above-mentioned monocoordinate model.

Another justification for this approach is that the photosynthetic antennae are unlikely to have a perfectly ordered structure. In Fig. 4 we have given the distribution of hopping times relative to the hopping in the perfect lattice, if the site coordinates can fluctuate randomly around the ideal lattice site with deviations given by a Gaussian distribution. A moderate fluctuation (2–5%) can result in a remarkable reduction or increase in the hopping time. Thus, it is possible that some sites just "happen" to be closer to the RC and because of the sixth power dependence of transfer rate on the distance, display a strongly enhanced transfer rate.

In order to meet different structural assumptions we have carried out simulations with four different structures given in Fig. 5. It turns out that the model parameters, which determine the excitation transfer kinetics in the antenna (τ_{tf}^{a} and Δ_0), do not depend significantly on the different structural assumptions because the transfer and consequently also equilibration is very fast anyway. The third model parameters, τ_{tf}^{RC}, which determines the overall trapping time of the excitation, varies quite a lot from structure to structure in order to satisfy the experimentally measured lifetimes (Table 1).

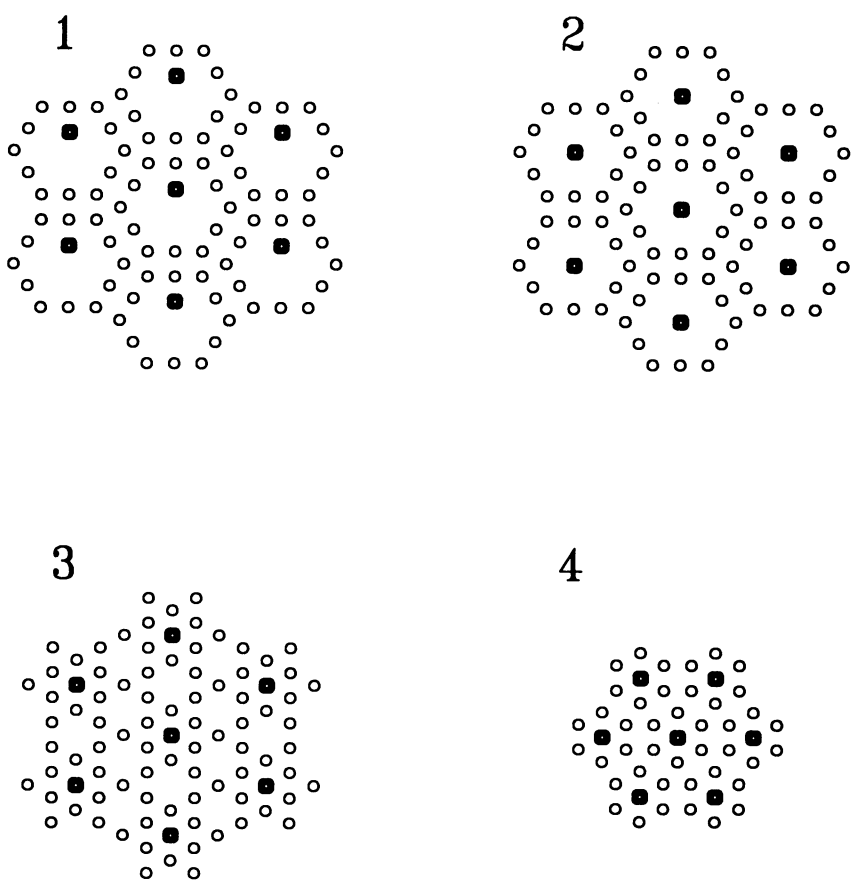

FIGURE 5 The model lattices used for simulations. The filled circles are the RCs. 1–3 have 12 sites in a PSU; 4 has 6 sites. 1 represents the monocoordinate RC case.

TABLE 1 Values of the model parameter τ_{tf}^{RC*} for four model structures in Fig. 5, which give experimentally observable lifetimes of antenna excitation—60 and 200 ps for open and closed RCs, respectively

RC state	1	2	3	4
Open (ps)	5	30	20	50
Closed (ps)	30	200	130	280

* τ_{tf}^{RC} is the transfer time from the antenna sites which are the closest to the RC.

Structures in which a number of RCs are situated closely side-by-side have also been proposed in the literature (Joliot et al., 1989). We will not address these possibilities here. We only note that our main conclusions about excitation transfer dynamics in inhomogeneous antenna would not be different for these structures, apart from the value extracted for τ_{tf}^{RC}.

The inner structure of the lattice site (B820, *e.g.*), which is not considered here, would further complicate the model, but this analysis must wait more detailed and reliable structural information.

Comparison with the experiment

In transient absorption experiments, the blue edge of the absorption band was excited (870 nm), and the kinetics were analyzed at several wavelengths (near the isosbestic point with a wavelength interval of 0.5 nm, otherwise 3–5 nm) over the whole band.

The traces at the blue side were dominated by the decay of induced absorption, whereas the simulations predict the existence of an initial fast bleaching component on the order of the τ_h, due to the directly excited pigments. Only after downhill energy transfer has taken place, can the induced absorption due to the pigments situated more to the red relative to the originally excited pigments be observed in the blue part of the spectrum. The absence of this component in the experimental traces implies that the initial downhill transfer must be fast enough to be entirely washed out by the convolution with the apparatus response, and this sets a higher limit to the τ_h of about 3 ps.

Within a narrow region (≈5 nm) around the isosbestic point of absorbance changes related to the ≈200 ps quenching time of closed RC (Fig. 6), a fast component is clearly resolved in the experimental transient absorption changes. A straightforward comparison with the simulations shows that if the inhomogeneous distribution function is chosen to be too broad, this region becomes too wide to fit to the experiment. This yields an upper limit for the FWHM of IDF of 10–15 nm. The third model parameter, the transfer time from the antenna to the RC, does not depend significantly on the previous two and can be estimated from the overall trapping time. In summary, for the absorption experiment a good fit is possible if τ_h is short (≈1 ps) and IDF is narrow (≤10 nm).

On the other hand, it was found to be difficult to fit the rising component of the fluorescence kinetics in the red wing

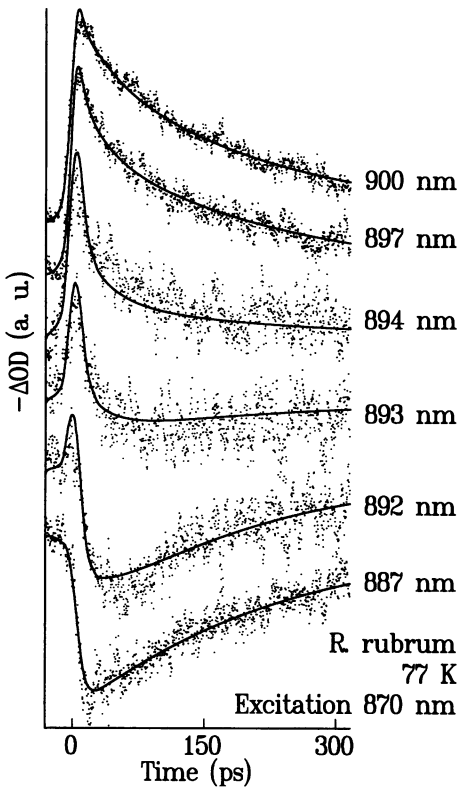

FIGURE 6 Comparison of theoretical absorption kinetics (*solid line*) with the experiment (*dots*) at 77 K. RCs are in the closed (P photooxidized) state. The same model parameters as in Figs. 1 and 2 are used.

of the emission spectrum ($\lambda \geq 920$ nm) assuming too fast hopping times and too narrow IDF.

After an extensive search of a simultaneous best fit for both absorption and fluorescence kinetics over the whole absorption and fluorescence bands, we achieved a satisfactory result for the following values of the adjustable parameters: $\tau_{tf}^{a} = 15$ ps, which gives for the residence time on an antenna lattice site ≈3 ps; $\Delta_0 = 10$ nm (120 cm^{-1}), which gives for the FWHM of the homogeneous spectrum 22 nm (260 cm^{-1}) at 77 K and 38 nm (470 cm^{-1}) at room temperature; τ_{tf}^{RC} values for different structures and RC states are given in Table 1. It can be seen that τ_{tf}^{RC} is directly related to the proportion of antenna molecules which are the nearest neighbors to the RC.

Figs. 6 and 7 represent 77 K experimental absorption and fluorescence decay curves together with the model ones that are convoluted with the experimental instrument response function in the case of closed RCs. We have used structure 1, which does not mean that we prefer this model over the other possible structures.

DISCUSSION

The calculated hopping time in this work is still considerably larger than that extracted from the annihilation data (Bakker et al., 1983; Van Grondelle, 1985). However, the analysis of those experiments does not take into account the fundamental

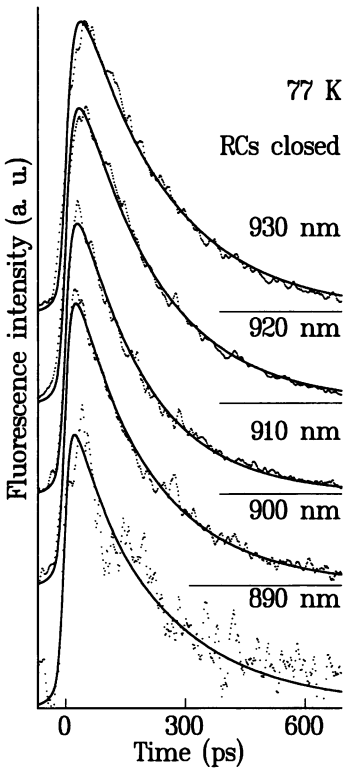

FIGURE 7 The same as Fig. 3 except for fluorescence. Excitation at 800 nm excites RC and antenna with equal probabilities. All antenna LHCs are initially equally excited.

inhomogeneity of antenna spectra, which should affect the conclusions, in particular at low temperature. To quantitatively evaluate and compare the interpretations of these different experimental approaches, one has to start from the same basic model assumptions. In our case this means a model in which specific assumptions have been made about the spectral inhomogeneity and antenna structure. The first step in that direction was made by Valkunas et al. (1992) using a macroscopic three-level approach that enables the qualitative description of the problem. A more thorough quantitative analysis on the microscopic level remains to be done.

Anyway, we can conclude that the hopping time in the antenna is on the order of a picosecond. It can be shown that neither the hopping time nor the charge separation rate in the RC can considerably improve the efficiency of the primary photosynthesis. Our results indicate that neither the migration in the antenna nor the trapping by the RC is the limiting factor and the true bottleneck of the process seems to be the transfer of excitation energy from the antenna to the RC, thereby supporting the earlier suggestion of Van Grondelle et al. (1988). This was measured for the first time by Bergström et al. (1989). More direct information on this point was obtained recently from measurements of the energy detrapping yield from the reaction center (K. Timpmann, F. G. Zhang, A. Freiberg, and V. Sundström. Detrapping of excitation energy from the reaction centre in the photosynthetic purple bacterium *Rhodospirillum rubrum*. *Biochim. Biophys. Acta*. submitted). Upon direct excitation of the photochemically active RC, 25 ± 5% of the excitation is transferred back to the LH antenna. A numerical simulation of the trapping dynamics compared with the measured kinetics and detrapping yield shows that energy transfer from the antenna to the reaction center is slow. It should be noted that this point was investigated in earlier work (Visscher et al., 1989) using the concept of the minor antenna form of the LH1. The antenna excited state lifetime of 30–40 ps measured after excitation of the red-most antenna pigments at 77 K was interpreted as the pairwise trapping time. This conclusion relies on the assumption that all the red-most antenna pigments are neighbors of the RC. In the concept of spectral inhomogeneity the red-most pigments may be everywhere in the antenna array and consequently also the pairwise trapping time cannot be directly deduced from the overall trapping time without knowing the antenna organization as can be seen from the Table 1. Furthermore, the possible distributions of the orientation factor χ^2, hopping time (see Figs. 3 and 4), and both antenna and RC transition energies (IDF), which all contribute to the pairwise trapping rate (Eq. 2), make the situation even more complicated, and the real pairwise trapping rate is likely to have a broad distribution.

The spectral position of the RC special pair of purple bacteria relative to that of the core antenna spectrum has been confusing for a long time. One has to note here that if the donor and acceptor are different species with different spectral properties (FWHM, Stokes shift), then the energy gap between them should not be calculated as the difference between the absorption maxima, but instead as the difference between the 0-0 transition positions. The latter may be found from the spectra, assuming that absorption and fluorescence bands show mirror symmetry relative to the 0-0 transition. This is not only a matter of definition but also a natural way of including these energy differences into the description, because in that case the detailed balance condition is satisfied for the back and forward transfer processes. One can easily check this by including the temperature dependence of the bandwidth (Eq. 5) explicitly into Eq. 4.

With this description of the energy gap, the above-mentioned problem can be solved. For example, in the case of *R. rubrum* the antenna and RC maxima at room temperature are 880 and 870 nm, respectively. The Stokes shifts are approximately 10 and 50 nm, which indicates that on average the RC has a 10 nm (110 cm^{-1}) lower energy than antenna despite the fact that its absorption maximum occurs at 10 nm higher energy. In reality the situation is probably even better because there is evidence that the RC absorbs at longer wavelengths in membranes than in isolated RCs (Kleinherenbrink et al., 1992).

At room temperature the primary electron donor of *Rps. viridis* RC in membranes is reported to have an absorption maximum at 980 nm (Kleinherenbrink et al., 1992), while that of the antenna is observed at 1015 nm. From the Stokes shift we calculate that the primary donor is at 15 nm (150 cm^{-1}, 200 K) higher energy than the antenna. Thus, at ambient temperatures where the real photosynthetic process

works, one would still expect an efficient energy transfer from antenna to the RC. Below 200 K, where the energy gap starts to exceed kT, the trapping efficiency should decrease rapidly. This is well in line with the observed temperature dependence of the integrated yield of fluorescence, which has a plateau at a higher temperature and starts to increase below 150 K (Deinum et al., 1992). However, this cannot explain the almost 50% quantum yield of charge separation at 6 K. It seems that in reality the primary electron donor in the membrane absorbs even more to the red than reported by Kleinherenbrink et al. (1992), and the low temperature bleaching band of the special pair measured in that work is possibly distorted by electrochromic shifts in the core antenna absorption upon charge separation.

There exists sufficient experimental evidence that a certain amount of static inhomogeneous broadening of optical spectra is a universal property, not only of low temperature solid solutions of relatively simple molecules (Avarmaa and Rebane, 1985) but also of complex biological systems (Reddy et al., 1992a). Whether or not there is in addition heterogeneity in the *R. rubrum* antenna, for instance the minor form proposed in earlier studies (Razjivin et al., 1982; Kramer et al., 1984a), is not clear. Jia et al. (1992) simulated the photosynthesis system I core antenna by deconvolving the whole broad spectrum into five to seven different spectral types (heterogeneity) of LHCs, each with an inhomogeneous spectral width of 200 cm^{-1}. They conclude that models in which the different spectral types are placed randomly and a single low energy species is placed close to the photochemical trap are consistent with experimental data on PSI. Some support for this approach comes from the molecular orbital calculations by Gudowska-Nowak et al. (1990), where large shifts in transition energies as a result of pigment conformation and pigment-protein interactions are calculated for BChl *a*.

We cannot exclude such a possible heterogeneity in the case of *R. rubrum*. We only note that all experimental data known to us are well described by the concept of inhomogeneous broadening. At the same time we were also able to obtain a reasonable fit to experimental data assuming that the pigment connecting the antenna and the RC is the red-most (heterogeneity), whereas the other pigments were randomly distributed over the IDF (inhomogeneity). In that case only the transfer time from antenna to RC had to be increased considerably. Also the dissociation of B880 into the B820 subunit form indirectly supports the idea that there exists only inhomogeneity, because otherwise one would expect the dissociation into several forms with different spectral properties, which is not observed experimentally (Chang et al., 1990, Van Mourik et al., 1991; Visschers et al., 1991).

In their hole-burning study of *Rb. sphaeroides*, Reddy et al. (1992b) burned narrow permanent zero-phonon holes in the red edge of the LH1 absorption band. In addition to the zero-phonon hole, a broad hole roughly corresponding to the width of the absorption band appears. The authors favor the interpretation that the zero-phonon hole is due to the lowest energy level of the B875 exciton band, very similar to their interpretation of the hole-burning spectrum of the Bchl *a*-protein from *Prosthecochloris aestuarii* (Johnson and Small, 1991). Uncorrelated coupling to the higher excitonic states combined with lifetime broadening of these upper exciton states is proposed to be the origin of the accompanying broad hole. Also in our case one could interpret the fast lifetime as the relaxation from the higher excitonic states to the lower ones. Nevertheless, we note that the excitonic model is not consistent with site-selected emission experiments (Van Mourik et al., 1992), which give a broad fluorescence band even exciting into the very red edge of the absorption band. In the excitonic model one would expect a significant line narrowing in that case. We propose here another possible interpretation that is consistent with both the hole-burning data of Reddy et al. (1992b) and the kinetic analysis presented in this paper.

The electron-phonon coupling of the protein-chlorophyll complexes in antenna systems is generally assumed to be weak. On the other hand for the RC special pair (a Bchl dimer), a strong electron-phonon coupling (Huang-Rhys factor $S \approx 3$) is estimated (for review see Reddy et al., 1992a). The elementary unit of LH1 is also a Bchl *a* dimer (Van Mourik et al., 1991), and we note that the hole-burning spectra of LH1 and RC special pair are remarkably similar. Therefore, we do not see a reason not to consider the possibility of significant electron-phonon coupling also in case of LH1. For the RC special pair the structure of the broad phonon sideband hole allowed a distinction between the low frequency internal vibration of the special pair and the protein phonons (Klevanik et al., 1988; Johnson et al., 1989). The former is assigned to a so-called "marker" mode, reflecting a mutual vibrational motion of the two special pair Bchl *a* molecules. Neither hole-burning (Reddy et al., 1992b) nor fluorescence site-selected spectra (Van Mourik et al., 1992) have revealed any specific feature that would confirm the existence of the marker mode in LH1. However, the recent site-selected fluorescence study of the B820 subunit (Visschers et al., 1993) have revealed that the anti-Stokes emission of B820 deviates significantly from the Urbach rule in the case of red-wing excitation. That may indicate the coupling to a 50–60 cm^{-1} vibration analogous to the RC marker mode.

By using the model by Johnson et al. (1991), we have simulated the homogeneous spectra at 0 K in the case of the linear Frank-Condon coupling of the electronic state to both the protein phonons and a local vibration. In that case the absorption profile of a single site with a 0-0 transition frequency of ν can be written as

$$L(\Omega - \nu) = \sum_{j=0}^{\infty} \frac{S_\nu^j e^{-S_\nu}}{j!} \left[e^{-S} \ell_0^{\,j}(\Omega - \nu - j\omega_\nu) + \sum_{i=1}^{\infty} \frac{S^i e^{-S}}{i!} \ell_i^{\,j}(\Omega - \nu - i\omega_{ph} - j\omega_\nu) \right], \quad (7)$$

where i and j run over the Franck-Condon progressions of phonons and a vibration, respectively. If $j = 0$, ℓ_0 represents the sharp Lorentzian zero phonon line and ℓ_i can be found

by convoluting ℓ_{i-1} with a one-phonon profile. Analogously ℓ_i^j can be found by convoluting ℓ_i^{j-1} with a one-vibration profile. S and S_ν are the so-called Huang-Rhys factors for phonons and a vibration, respectively. ω_{ph} and ω_ν give the mean frequencies of the phonons and a vibration. The generalization of this equation to more than one vibration is straightforward.

In Fig. 8 we have given the most characteristic results of simulations. It can be shown that if the width of the one-vibration profile is comparable to the frequency of the vibration, then it will not show up as a distinct feature in the spectrum, and we can get spectra very similar to those observed experimentally. If this width is too narrow, we will get a vibronic Franck-Condon progression of quite narrow zero-phonon lines, which would have been seen in the experiment. The width of the one-vibration profile has two different physical meanings. First of all, it is the uncertainty broadening due to the fast vibrational relaxation: 100 fs relaxation time would correspond to the width of 50 cm^{-1}. Also the possible (inhomogeneous) distribution of vibrational frequencies of different antenna sites may contribute to the width. It should be noted that in the case of the RC the later contribution seems to be negligible because as it was shown by Reddy et al. (1993) that inhomogeneous broadening originates in the RC special pair primarily from statistical fluctuations in protein structure around the special pair rather than from a distribution of structures for the special pair itself.

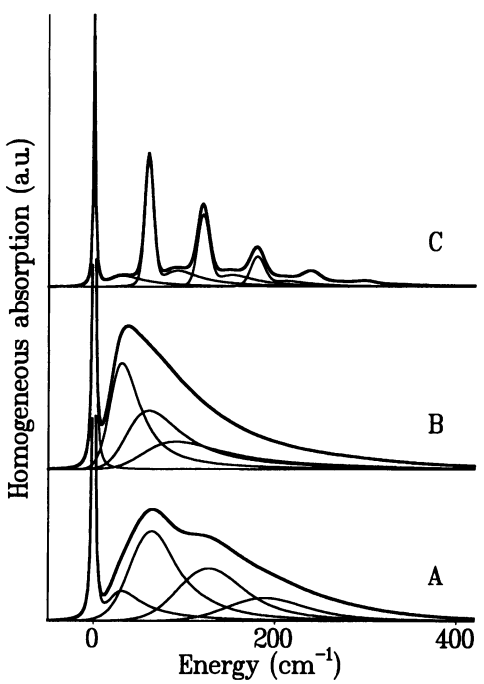

FIGURE 8 Homogeneous electron-phonon spectra. The sharp zero-phonon line has a Lorentzian shape. The one-phonon profile is described by the asymmetric profile with a Gaussian and a Lorentzian shape for the low and high energy halves of the profile, respectively. The one-vibration profile is taken as a Gaussian shape. In each case the four first profiles of the most significant Franck-Condon progression are presented together with the overall absorption. Parameters: for the one phonon profile the Gaussian and Lorentzian half-widths are 15 and 25 cm^{-1}, respectively, which gives the total width of 40 cm^{-1}; phonon and vibration frequencies are 30 and 60 cm^{-1}, respectively; the total electron phonon coupling factor S is 2. (A) S is 0.5 and 1.5 for phonons and vibration, respectively; the width of the one-vibration profile is 50 cm^{-1}. (B) S for phonons is 2, not any coupling to the local vibration. (C) The same as A, but the width of the one-vibration profile is 10 cm^{-1}.

Van Mourik et al. (1992) simulated the fluorescence polarization and site-selected emission spectra using a twice as large inhomogeneous distribution width (20 nm) as estimated here to obtain good agreement with the experiment. It can be shown that a good fit to these experimental results may be gained also by assuming a narrower IDF in combination with broader homogeneous spectra, such as used by Avarmaa et al. (1986) and proposed by us above to interpret the hole-burning results. In that case one can also easily reproduce the broad emission spectrum observed upon excitation into the red wing of the absorption spectrum.

It should also be noted that for the Förster mechanism to be valid, vibrational relaxation within the excited state would have to be faster than the single-step transfer time—in our case on the order of 1 ps. The damping time for low frequency protein phonons, which are coupled to the electronic transition of the pigments and play the major role in our case, is not well established yet but may be of the same order or even longer. In that case more sophisticated quantum mechanical approaches should be applied (e.g., Jean et al., 1991, 1992). However, these methods (e.g., the multilevel Redfield theory) are far too crude yet to enable direct comparison with experiment. We also note that we have not seen any oscillatory behavior in our observables, which would have directly indicated the presence of the above-mentioned problem.

In earlier work Pullerits and Freiberg (1992) concluded that the broad homogeneous spectrum of the special pair may be important in making the energy transfer from the antenna to the RC sufficiently efficient also in the case of a significant spectral disorder (inhomogeneity). That conclusion and the discussion above about the possible strong electron-phonon coupling in LH1 can shed some light on why the elementary unit of the core antenna is a dimer. The dimeric nature seems to increase the electron-phonon coupling significantly, which broadens the spectrum and makes the excitation energy transfer independent of the inevitable spectral inhomogeneity of pigment-protein complexes. In the case of B800, there is no need for excitation transfer within the spectral band and the elementary unit is a monomer (Kramer et al., 1984b) with weak electron-phonon coupling (Reddy et al., 1992a). In LH1, where excitation transfer takes place within the inhomogeneously broadened band, the dimeric nature guarantees sufficient spectral overlap and efficient transfer even from the redmost pigments.

In the analysis of the "optimization factors" of photosynthesis (Fetisova et al., 1985) mainly the strategy of choosing the most favorable possibilities is considered. It seems that the other case—the strategy of avoiding the least favorable possibilities—is also widespread in photosynthesis. In this article we have pointed out two of these possibilities: keeping

the transition dipole moments in the membrane plane avoids a major amount of possible conformations with very small orientational factors (see Fig. 3), and the possible enhanced electron-phonon coupling in LH1 prevents the excitation from being trapped by the red molecules of the antenna inhomogeneous distribution.

CONCLUSIONS

We have presented a simultaneous modeling of picosecond absorption and fluorescence kinetics. Our empirical approach has resulted in a good fit to the experimental data. One of the major conclusions is that owing to spectral inhomogeneity three distinct features arise in the kinetics of excitation trapping: (1) fast local equilibration with time constants of $\tau_h \approx 2$–3 ps; (2) excitation transfer between local minima with time constants ≈ 30 ps; and (3) transfer to the RC followed by charge separation. Some of the details of the modeling results are still obscured by the limited resolution of the experiments and have to be verified in the future.

We thank Prof. L. Valkunas for valuable discussions.
This research was supported by the EEC Contract SC1*-CT92-0796. T.P. acknowledges the support from the Swedish NFR and EMBO.

REFERENCES

Avarmaa, R. A., and K. K. Rebane. 1985. High-resolution optical spectra of chlorophyll molecules. *Spectrochim. Acta Part A Mol. Spectrosc.* 41: 1365–1380.

Avarmaa, R., R. Jaaniso, K. Mauring, I. Renge, and R. Tamkivi. 1986. Influence of energy transfer on the structure of site-selection spectra of molecules. *Mol. Phys.* 57:605–621.

Bakker, J. G. C., R. van Grondelle, and W. Th. F. den Hollander. 1983. Trapping, loss and annihilation of excitations in a photosynthetic system. II. Experiments with the purple bacteria *Rhodospirillum rubrum* and *Rhodopseudomonas capsulatus*. *Biochim. Biophys. Acta.* 725:508–518.

Beauregard, M., I. Martin, and A. F. Holzwarth. 1991. Kinetic modelling of exciton migration in photosynthetic systems. (1) Effects of pigment heterogeneity and antenna topography on exciton kinetics and charge separation yields. *Biochim. Biophys. Acta.* 1060:271–283.

Bergström, H., R. van Grondelle, and V. Sundström. 1989. Characterization of excitation energy trapping in photosynthetic purple bacteria at 77 K. *FEBS Lett.* 250:503–508.

Boonstra, A. F., R. W. Visschers, F. Caalkoen, R. van Grondelle, E. F. J. van Bruggen, and E. J. Boekema. 1993. Structural characterization of the B800–850 and B875 light-harvesting antenna complexes from *Rhodobacter sphaeroides* by electron microscopy. *Biochim. Biophys. Acta.* 1142:181–188.

Breton, J. 1985. Orientation of the chromophores in the reaction center of *Rhodopseudomonas viridis*. Comparison of low-temperature linear dichroism spectra with a model derived from X-ray crystallography. *Biochim. Biophys. Acta.* 810:235–245.

Chang, M. C., P. M. Callahan, P. S. Parkes-Loach, T. M. Cotton, and P. A. Loach. 1990. Spectroscopic characterization of the light-harvesting complex of *Rhodospirillum rubrum* and its structural subunit. *Biochemistry.* 29:421–429.

Deinum, G., T. J. Aartsma, R. van Grondelle, and J. Amesz. 1989. Singlet-singlet excitation annihilation measurements in the antenna of *Rhodospirillum rubrum* between 300 and 4 K. *Biochim. Biophys. Acta.* 976:63–69.

Deinum, G., F. A. M. Kleinherenbrink, T. J. Aartsma, and J. Amesz. 1992. The fluorescence yield of *Rhodopseudomonas viridis* in relation to the redox state of the primary electron donor. *Biochim. Biophys. Acta.* 1099: 81–84.

Den Hollander, W. T. F., J. G. C. Bakker, and R. van Grondelle. 1983. Trapping, loss and annihilation of excitations in a photosynthetic system. I. Theoretical aspects. *Biochim. Biophys. Acta.* 725:508–518.

Duysens, L. N. M. 1986. Introduction to (bacterio)chlorophyll emission: a historical perspective. *In* Light Emission by Plants and Bacteria. Govindjee, J. Amesz, and D. C. Fork, editors. Academic Press, Inc., Orlando, FL. 3–28.

Fetisova, Z. G., A. Yu. Borisov, and M. V. Fok. 1985. Analysis of structure-function correlations in light-harvesting photosynthetic antenna: structure optimization parameters. *J. Theor. Biol.* 112:41–75.

Förster, Th. 1965. Delocalized excitation and excitation transfer. *In* Modern Quantum Chemistry. Vol. III. O. Sinanoglu, editor. Academic Press, Inc., New York. 93–137.

Freiberg, A., V. I. Godik, T. Pullerits, and K. Timpmann. 1989. Picosecond dynamics of directed excitation transfer in spectrally heterogeneous light-harvesting antenna in purple bacteria. *Biochim. Biophys. Acta.* 973: 93–104.

Freiberg, A., V. I. Godik, and K. Timpmann. 1987. Spectral dependence of the fluorescence lifetime of *Rhodospirillum rubrum*. Evidence for inhomogeneity of B880 absorption band. *In* Progress in Photosynthesis Research. Vol. 1. J. Biggins, editor. Martinus Nijhoff, Dordrecht, The Netherlands. 45–48.

Freiberg, A., and T. Pullerits. 1990. Energy transfer and trapping in spectrally disordered photosynthetic membranes. *In* Reaction Centers of Photosynthetic Bacteria. M.-E. Michel-Beyerle, editor. Springer-Verlag, Berlin. 339–348.

Ghosh, R., and R. Bachofen. 1989. Die molekulare Struktur der photosynthetischen Membranen bei anoxygenen phototropen Bakterien. *Forum Mikrobiol.* 12:556–564.

Gingras, G., and R. Picorel. 1990. Supramolecular arrangement of *Rhodospirillum rubrum* B880 holochrome as studied by radiation inactivation and electron paramagnetic resonance. *Proc. Natl. Acad. Sci. USA.* 87: 3405–3409.

Gudowska-Nowak, E., M. D. Newton, and J. Fajer. 1990. Conformational and environmental effects on bacteriochlorophyll optical spectra: correlations of calculated spectra with structural results. *J. Phys. Chem.* 94: 5795–5801.

Holzwarth, A. R. 1991. Excited state kinetics in chlorophyll systems and its relationship to the functional organization of the photosystems. *In* The Chlorophylls. H. Scheer, editor. CRC Handbook, CRC Press, Boca Raton, FL. 1125–1152.

James, D. R., and W. R. Ware. 1985. A fallacy in the interpretation of fluorescence decay parameters. *Chem. Phys. Lett.* 120:455–459.

Jean, J. M., C.-K. Chan, G. R. Fleming, and T. G. Owens. 1989. Excitation transport and trapping on spectrally disordered lattices. *Biophys. J.* 56: 1203–1215.

Jean, J. M., G. R. Fleming, and R. A. Friesner. 1991. Classical and quantum models of activationless reaction dynamics. *Ber. Bunsenges. Phys. Chem.* 95:253–258.

Jean, J. M., R. A. Friesner, and G. R. Fleming. 1992. Application of a multilevel Redfield theory to electron transfer in condensed phases. *J. Chem. Phys.* 96:5827–5842.

Jia, Y., J. M. Jean, M. M. Werst, C.-K. Chan, and G. R. Fleming. 1992. Simulations of the temperature dependence of energy transfer in the PSI core antenna. *Biophys. J.* 63:259–273.

Johnson, S. G., I.-J. Lee, and G. J. Small. 1991. Solid state spectral line-narrowing spectroscopies. *In* The Chlorophylls. H. Scheer, editor. CRC Handbook, CRC Press, Boca Raton, FL. 739–768.

Johnson, S. G., and G. J. Small. 1991. Excited state structure and energy transfer dynamics of the Bacteriochlorophyll *a* antenna complex from *Prosthecochloris aestuarii*. *J. Phys. Chem.* 95:471–479.

Johnson, S. G., D. Tang, R. Jankowiak, J. M. Hayes, G. J. Small, and D. M. Tiede. 1989. Structure and marker mode of the primary electron donor state absorption of photosynthetic bacteria: hole-burned spectra. *J. Phys. Chem.* 93:5953–5957.

Joliot, P., A. Verméglio, and A. Joliot. 1989. Evidence for supercomplexes between rection centers, cytochrome c_2 and cytochrome bc_1 complex in *Rhodobacter sphaeroides* whole cells. *Biochim. Biophys. Acta.* 975: 336–345.

Källebring, B., and Ö. Hansson. 1991. A theoretical study of the effect of charge recombination on the transfer and trapping of excitation energy in photosynthesis. *Chem. Phys.* 149:361–372.

Kleinherenbrink, F. A. M., G. Deinum, S. C. M. Otte, A. J. Hoff, and J. Amesz. 1992. Energy transfer from lon-wavelength absorbing antenna bacteriochlorophylls to the reaction center. *Biochim. Biophys. Acta*. 1099: 175–181.

Klevanik, A. V., A. O. Ganago, A. Ya. Shkuropatov, and V. A. Shuvalov. 1988. Electron-phonon and vibronic structure of absorption spectra of the primary electron donor in reaction centers of *Rhodopseudomonas viridis, Rhodobacter sphaeroides* and *Chloroflexus aurantiacus* at 1.7–70 K. *FEBS Lett*. 237:61–64.

Kramer, H. J. M., J. D. Pennoyer, R. van Grondelle, W. H. J. Westerhuis, R. A. Niederman, and J. Amesz. 1984a. Low temperature optical properties and pigment organization of the B875 light-harvesting bacteriochlorophyll protein complex of purple photosynthetic bacteria. *Biochim. Biophys. Acta*. 767:335–344.

Kramer, H. J. M., R. van Grondelle, C. N. Hunter, W. H. J. Westerhuis, and J. Amesz. 1984b. Pigment organization of the B800–850 antenna complex of *Rhodobacter sphaeroides. Biochim. Biophys. Acta*. 765:156–165.

Krauss, N., W. Hinrichs, I. Witt, P. Fromme, W. Pritzkow, Z. Dauter, C. Betzel, K. S. Wilson, H. T. Witt, and W. Saenger. 1993. Three-dimensional structure of system I of photosynthesis at 6 Å resolution. *Nature (Lond.)*. 361:326–330.

Kudzmauskas, S., L. Valkunas, and A. Yu. Borisov. 1983. A theory of excitation transfer in photosynthetic units. *J. Theor. Biol*. 105: 13–23.

Kühlbrandt, W., and D. N. Wang. 1991. Three-dimensional structure of plant light-harvesting complex determined by electron crystallography. *Nature (Lond.)*. 350:130–134.

Meckenstock, R. U., R. A. Brunisholz, and H. Zuber. 1992a. The light-harvesting core-complex and the B820-subunit from *Rhodopseudomonas marina*. Part I. Purification and characterisation. *FEBS Lett*. 311: 128–134.

Meckenstock, R. U., R. A. Brunisholz, and W. Zuber. 1992b. The light-harvesting core-complex and the B820-subunit from *Rhodopseudomonas marina*. Part II. Electron microscopic characterisation. *FEBS Lett*. 311: 135–138.

Miller, J. F., S. B. Hinchigeri, P. S. Parkes-Loach, P. M. Callahan, J. R. Sprinkle, J. R. Riccobono, and P. A. Loach. 1987. Isolation and characterization of a subunit form of the light-harvesting complex of *Rhodospirillum rubrum. Biochemistry*. 26:5055–5062.

Miller, K. R. 1982. Three-dimensional structure of a photosynthetic membrane. *Nature (Lond.)*. 300:53–55.

Ormos, P., A. Ansari, D. Braunstein, B. R. Cowen, H. Frauenfelder, M. K. Hong, I. E. T. Iben, T. B. Sauke, P. J. Steinbach, and R. D. Young. 1990. Inhomogeneous broadening in spectral bands of carbonmonoxymyoglobin. The connection between spectral and functional heterogeneity. *Biophys. J*. 57:191–199.

Osad'ko, I. S. 1979. Determination of electron-phonon coupling from structured optical spectra of impurity centers. *Sov. Phys. Usp*. 22: 311–329.

Pearlstein, R. M. 1982. Exciton migration and trapping in photosynthesis. *Photochem. Photobiol*. 35:835–844.

Pearlstein, R. M. 1992a. Theory of the optical spectra of the bacteriochlorophyll *a* antenna protein trimer from *Prosthecochloris aestuarii. Photosynth. Res*. 31:213–226.

Pearlstein, R. M. 1992b. Kinetics of exciton trapping by monocoordinate reaction centers. *J. Lumin*. 51:139–147.

Picorel, R., A. L'Ecuyer, M. Potier, and G. Gingras. 1986. Structure of the B880 holochrome of *Rhodospirillum rubrum* as studied by the radiation inactivation method. *J. Biol. Chem*. 261:3020–3024.

Pullerits, T., and A. Freiberg. 1991. Picosecond fluorescence of simple photosynthetic membranes: evidence of spectral inhomogeneity and directed energy transfer. *Chem. Phys*. 149:409–418.

Pullerits, T., and A. Freiberg. 1992. Kinetic model of primary energy transfer and trapping in photosynthetic membranes. *Biophys. J*. 63: 879–896.

Razjivin, A. P., R. V. Danielius, R. A. Gadonas, A. Yu. Borisov, and A. S. Piskarskas. 1982. The study of excitation transfer between light-harvesting antenna and reaction center in chromatophores from purple bacterium *Rhodospirillum rubrum* by selective picosecond spectroscopy. *FEBS Lett*. 143:40–44.

Rebane, K. K. 1970. Impurity spectra of solids. Plenum Press, New York.

Reddy, N. R. S., P. A. Lyle, and G. J. Small. 1992a. Applications of spectral hole burning spectroscopy to antenna and reaction center complexes. *Photosynth. Res*. 31:167–194.

Reddy, N. R. S., R. Picorel, and G. J. Small. 1992b. B896 and B870 components of the *Rhodobacter sphaeroides* antenna: a hole burning study. *J. Phys. Chem*. 96:6458–6464.

Reddy, N. R. S., S. V. Kolaczkowski, and G. J. Small. 1993. A photoinduced persistent structural transformation of the special pair of a bacterial reaction center. *Science (Wash. DC)*. 260:68–71.

Ries, B., H. Bässler, M. Grünewald, and B. Movaghar. 1988. Monte Carlo study of relaxation and diffusion in glassy systems. *Phys. Rev. B*. 37: 5508–5517.

Seely, G. R. 1973. Effects of spectral variety and molecular orientation on energy trapping in the photosynthetic unit: a model calculation. *J. Theor. Biol*. 40:173–187.

Shipman, L. L. 1980. Excitation migration in photosynthetic systems on the picosecond timescale. *Photochem. Photobiol*. 31:157–167.

Stark, W., W. Kühlbrandt, I. Wildhaber, E. Wehrli, and K. Mühlethaler. 1984. The structure of the photoreceptor unit of *Rhodopseudomonas viridis. EMBO J*. 3:777–783.

Sundström, V., and R. van Grondelle. 1991. Dynamics of excitation energy transfer in photosynthetic bacteria. *In* The Chlorophylls. H. Scheer, editor. CRC Handbook, CRC Press, Boca Raton, FL. 1097–1124.

Sundström, V., R. van Grondelle, H. Bergström, E. Åkesson, and T. Gillbro. 1986. Excitation energy transport in the bacteriochlorophyll antenna systems of *Rhodospirillum rubrum* and *Rhodobacter sphaeroides* studied by low-intensity picosecond spectroscopy. *Biochim. Biophys. Acta*. 851: 431–446.

Timpmann, K., A. Freiberg, and V. I. Godik. 1991. Picosecond kinetics of light excitations in photosynthetic purple bacteria in the temperature range of 300–4 K. *Chem. Phys. Lett*. 182:617–622.

Valkunas, L., F. van Mourik, and R. van Grondelle. 1992. On the role of spectral and spatial antenna inhomogeneity in the process of excitation energy trapping in photosynthesis. *J. Photochem. Photobiol. B: Biol*. 15: 159–170.

Van Grondelle, R. 1985. Excitation energy transfer, trapping and annihilation in photosynthetic systems. *Biochim. Biophys. Acta*. 811: 147–195.

Van Grondelle, R., H. Bergström, V. Sundström, and T. Gillbro. 1987. Energy transfer within the bacteriochlorophyll antenna of purple bacteria at 77 K, studied by picosecond absorption recovery. *Biochim. Biophys. Acta*. 894:313–326.

Van Grondelle, R., H. Bergström, V. Sundström, R. J. van Dorssen, M. Vos, and C. N. Hunter. 1988. Excitation energy transfer in the light-harvesting antenna of photosynthetic purple bacteria: the role of the long-wavelength absorbing pigment B896. *In* Photosynthetic Light-Harvesting Systems. H. Scheer, and S. Schneider, editors. Walter de Gruyter, Berlin, New York. 519–530.

Van Mourik, F. 1993. Spectral inhomogeneity of the bacterial light-harvesting antennae: causes and consequences. Ph.D. thesis. Amsterdam, The Netherlands. 128 pp.

Van Mourik, F., C. J. R. van der Oord, K. J. Visscher, P. S. Parkes-Loach, P. A. Loach, R. W. Visschers, and R. van Grondelle. 1991. Exciton interactions in the light-harvesting antenna of photosynthetic bacteria studied with triplet-singlet spectroscopy and singlet-triplet annihilation. *Biochim. Biophys. Acta*. 1059:111–119.

Van Mourik, F., R. W. Visschers, and R. van Grondelle. 1992. Energy transfer and aggregate size effects in the inhomogeneously broadened core light-harvesting complex of *Rhodobacter sphaeroides. Chem. Phys. Lett*. 193:1–7.

Van Mourik, F., K. J. Visscher, J. M. Mulder, and R. van Grondelle. 1993. Spectral inhomogeneity of the light-harvesting antenna of *Rhodospirillum rubrum* probed by T-S spectroscopy and singlet-triplet annihilation at low temperatures. *Photochem. Photobiol*. 57:19–23.

Visscher, K. J., H. Bergström, V. Sundström, C. N. Hunter, and R. van Grondelle. 1989. Temperature dependence of energy transfer from the long wavelength antenna Bchl-896 to the reaction center in *Rhodospirillum rubrum, Rhodobacter sphaeroides* (w.t. and M21 mutant) from 77 K to 177 K, studied by picosecond absorption spectroscopy. *Photosynth. Res*. 22:211–217.

Visschers, R. W. 1993. Subunit structure and protein interactions in antenna complexes of purple non-sulphur bacteria. Ph.D. thesis. Amsterdam, The Netherlands. 131 pp.

Visschers, R. W., M. C. Chang, F. van Mourik, P. S. Parkes-Loach, B. A. Heller, P. A. Loach, and R. van Grondelle. 1991. Fluorescence polarization and low-temperature absorption spectroscopy of a subunit form of light-harvesting complex I from purple photosynthetic bacteria. *Biochemistry*. 30:5734–5742.

Visschers, R. W., F. van Mourik, R. Monshouwer, and R. van Grondelle. 1993b. Inhomogeneous spectral broadening of the B820 subunit form of LH1. *Biochim. Biophys. Acta*. 1141:238–244.

Vos, M., R. van Grondelle, F. W. van der Kooy, D. van de Poll, J. Amesz, and L. N. M. Duysens. 1986. Singlet-singlet annihilation at low temperatures in the antenna of purple bacteria. *Biochim. Biophys. Acta*. 850: 501–512.

Welte, W., and W. Kreutz. 1982. Formation, structure and composition of a planar hexagonal lattice composed of specific protein-lipid complexes in the thylakoid membranes of *Rhodopseudomonas viridis*. *Biochim. Biophys. Acta*. 692:479–488.

Zhang, F. G., T. Gillbro, R. van Grondelle, and V. Sundström. 1992. Dynamics of energy transfer and trapping in the light-harvesting antenna of *Rhodopseudomonas viridis*. *Biophys. J*. 61:694–703.